Kinetics and Catalysis, Vol. 46, No. 5, 2005, pp. 736–742. Translated from Kinetika i Kataliz, Vol. 46, No. 5, 2005, pp. 780–786.
Original Russian Text Copyright © 2005 by Gordeeva, Gubar', Plyasova, Malakhov, Aristov.

Composite Water Sorbents of the Salt in Silica Gel Pores Type: The Effect of the Interaction between the Salt and the Silica Gel Surface on the Chemical and Phase Compositions and Sorption Properties

L. G. Gordeeva, A. V. Gubar', L. M. Plyasova, V. V. Malakhov, and Yu. A. Aristov

Boreskov Institute of Catalysis, Siberian Division, Russian Academy of Sciences, Novosibirsk, 630090 Russia

Received October 13, 2004

Abstract—The influence of the inorganic salt–silica gel surface interaction on the chemical and phase compositions and sorption properties of composites of the salt in silica gel pores type is studied. Two possible interaction mechanisms are considered: (1) the ion-exchange adsorption of metal cations on the silica gel surface from a solution of a salt ($CaCl_2$, $CuSO_4$, $MgSO_4$, Na_2SO_4, and LiBr) and (2) the solid-phase spreading of a salt ($CaCl_2$) over the silica gel surface. The adsorption of metal cations on the silica gel surface in the impregnation step affords $\equiv Si–OM^{n+}$ surface complexes in the composites. As a result, two salt phases are formed in silica gel pores at the composite drying stage, namely, an amorphous phase on the surface and a crystalline phase in the bulk. The sorption equilibrium between the $CaCl_2/SiO_2$ system and water vapor depends on the ratio of the crystalline phase to the amorphous phase in the composite.

INTRODUCTION

It is well known that the properties of composite systems can differ substantially from the sum of the properties of the components [1, 2]. Indeed, dispersing inorganic salts (sulfates, chlorides, and bromides of alkaline and alkaline-earth metals) to nanosizes by incorporating them into pores of matrices (mesoporous and microporous silica gels, γ-alumina, porous carbon materials, etc.) can affect their sorption equilibrium with water vapor, the melting points of their crystalline hydrates, and their phase composition [3–6]. Two factors can change the properties of the salts: (1) salt dispersion in pores to nanosizes ("size effect") and (2) interaction between the salt and the matrix.

When the salt content is higher than 20 wt %, the structure and adsorption properties of the salt-in-porous-matrix composites depend most strongly on the salt particle size, which, in turn, is determined by the porous structure of the matrix [3, 7, 8]. In other words, the size effect appears. Indeed, the dispersion of the salt in pores with an average diameter of $d_p \approx 15$ nm and above affords a crystalline phase of the salt with a crystallite size comparable to the pore diameter. The sorption of water vapor by such systems first results in crystalline hydrates of the salt and then affords a solution of the salt in pores [5–8], as in the case of a bulky salt. In smaller pores of size 6–8 nm, an X-ray amorphous salt phase forms (the size of the coherently scattering region is $d_{coh} < 5$ nm) [7–9]. No crystalline hydrates are formed upon vapor sorption by such systems, and the composition of the hydrated salt changes monotonically. This behavior is characteristic of solutions of salts or crystalline hydrates with a "vacancy" structure [10]. It turned out that, for salt contents above 20 wt %, the influence of the chemical nature of the matrix and of the interaction between the matrix surface and the salt is of secondary importance [7, 8].

For the salt content of the matrix pores below 10–20 wt %, the interaction between the salt and the matrix surface affects the phase composition and sorption properties of the composite [11, 12]. Due to this interaction, an X-ray amorphous phase of the salt ($d_{coh} <$ 5 nm) is formed even in rather wide pores of the matrix. For instance, at a low salt content of the pores of KSK silica gel ($d_p \approx 15$ nm), no crystalline phase of the salt was observed. The composition of this system changes monotonically during vapor sorption, and no stable crystalline hydrates are formed in the pores. In this case, the formation of the X-ray amorphous phase is due to the interaction between the silica gel surface and the salt or its solution at the composite synthesis stage rather than to the size effect ($d_p > d_{coh}$).

The synthesis of salt-in-silica-gel-pores (SSGP) sorbents consists of two steps, specifically, matrix impregnation with an aqueous solution of a salt followed by thermal drying. An analysis demonstrated that the composite components can interact in both steps of the synthesis. In the impregnation step, the ion-exchange adsorption of metal cations on the silica gel surface occurs [13–15]. The drying step is accompanied by the so-called liquid-phase or solid-phase spreading of the salt over the silica gel surface [16, 17].

The surface silanol groups of silica gel are ionized in aqueous solutions of electrolytes:

0023-1584/05/4605-0736 © 2005 MAIK "Nauka/Interperiodica"

$$\equiv Si–OH \rightleftharpoons \equiv Si–O^- + H^+, \quad (I)$$

and metal cations are adsorbed on the surface:

$$\equiv Si–O^- + M^{n+} \rightleftharpoons \equiv Si–OM^{(n-1)+}, \quad (II)$$

$$\equiv Si–OH + M^{n+} \rightleftharpoons \equiv Si–OM^{(n-1)+} + H^+. \quad (III)$$

Furthermore, cations having a charge of 2 or above can form complexes in which the metal cation is bonded to two silanol groups of the surface:

$$2\equiv Si–OH + M^{n+} \rightleftharpoons 2(\equiv Si–O)M^{(n-2)+} + 2H^+. \quad (IV)$$

Another possible mechanism of surface complex formation can be the so-called surface-induced hydrolysis:

$$\equiv Si–OH + M^{n+} + H_2O \rightleftharpoons Si–OM^{(n-1)+}OH^- + 2H^+. \quad (V)$$

The resulting surface complexes can affect the chemical and phase compositions of the composite and its sorption equilibrium with water vapor.

The interaction between the salt and the matrix surface can occur at the thermal drying stage. As is demonstrated by experimental data and by thermodynamic analysis of the composite systems MX/Al_2O_3 and MX/SiO_2 (M = Li, Na, K, Rb, Cs; X = Cl, I, NO_3) [16, 17], if the energy of adhesion between the salt and the matrix surface (σ_a) is higher than the surface energy of the salt (σ_{MA}), then the calcination of a mechanical mixture of the components will be accompanied by the solid-phase or liquid-phase spreading of the salt over the matrix surface. The Coulomb and dispersion interactions between the surface ions of the salt and silica gel induce the disordering of the surface salt layers, resulting in an increase in the salt–matrix interfacial area and in some compensation for the surface energy of the system. As a result, the amorphous phase of the salt is formed on the oxide surface.

The purpose of this work is to study the influence of the ion-exchange adsorption of metal cations on the silica gel surface at the impregnation stage and of the solid-phase spreading of the salt over the silica gel surface at the drying stage on the chemical and phase compositions of the SSGP composites and on the SSGP–water vapor sorption equilibrium.

EXPERIMENTAL

KSK silica gel with a specific surface area of S_{sp} = 330 m^2/g, a pore volume of V_{sp} = 1.0 cm^3/g, and an average pore diameter of d_{av} = 15 nm was used as the host matrix.

The ion-exchange equilibrium between the silica gel surface and salt solutions was studied by potentiometric titration with an alkali at pH 2–9 [14]. Hydrochloric acid (1 N) was added to a suspension of prewashed silica gel (40–90 μm fraction) in a salt solution in twice distilled, CO_2-free water until the point of zero charge was achieved (pH 2–2.5 [13]). Thereafter, the suspension was titrated with 0.1 N NaOH to pH 9–9.5. The pH values of solutions were measured with an I-130 laboratory ion meter, using a glass electrode as the indicator and an Ag/AgCl electrode as the reference. The glass electrode was placed into the silica gel–containing solution to be examined, which was connected to a salt solution of the same concentration with a salt bridge. This solution was connected to the Ag/AgCl electrode using an electrolyte key. The measurements were carried out in nitrogen to prevent the dissolution of atmospheric CO_2 in the solution. Ionometric data were recorded 5–10 min after the titrant was added, when the reading of the ion meter varied at a rate of no higher than 0.2 mV/min. The charge of the silica gel surface as a function of pH was calculated from the difference between the titration curves of the suspension and the reference salt solution.

Composite materials were synthesized by the impregnation of silica gel with an aqueous salt solution followed by drying at 200–380°C [5]. The salt content of composites was determined by flame absorption spectroscopy.

Chemical analysis was carried out by the differentiating dissolution method [18]. To separate and analyze the phases of a composite, they were successively dissolved in different solvents. A weighed sample was placed in the flow reactor of a stoichiograph, and the composition of the solvent flow was successively changed from H_2O to 0.1 M HCl and then an HF solution (1 : 5). The solution leaving the reactor was directed to an analyzer (an ICP spectrometer) to determine the concentrations of metal, sulfur, and silicon. Next, the dissolution kinetics of these elements were plotted and stoichiometry calculations were carried out to determine the composition and phase makeup of the analyzed sample [19].

The phase composition of composites was determined by X-ray powder diffraction and differential scanning calorimetry. A D-500 diffractometer (Siemens) with a graphite reflected-beam monochromator was used. Measurements were carried out using CuK_α radiation in the scan mode (2θ = 5°–60°) with 0.02° 2θ increments and an accumulation time of 10 s at each point. Relative phase content was derived from the integrated intensity of the peak at 14.6° as a unit reflection without superposition, using a mechanical mixture of the silica gel and $CaCl_2 \cdot 2H_2O$ (14.1 wt %) as the reference.

Differential scanning calorimetry was carried out on a DSC 404 C Pegasus calorimeter (Netzsch) using the following procedure. A sample (20 mg) was saturated with vapor to a water content of N = 6 mol/(mol $CaCl_2$) and was sealed in a standard aluminum crucible. The crucible was placed in the calorimeter furnace. Measurements were carried out as follows: the sample was held at T = –30°C for 10 min, heated to 95°C, and cooled. The heating and cooling rates were 5 K/min. At least three cooling–heating cycles were accomplished. The results were processed using the Proteus Analysis standard software.

The sorption equilibrium between the resulting samples and water vapor was studied by thermogravim-

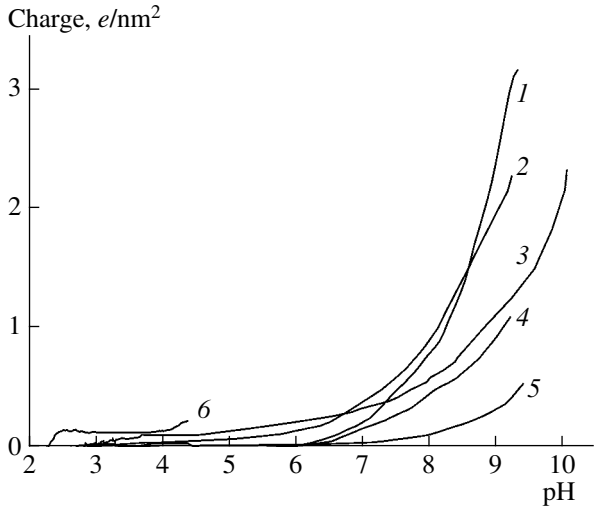

Fig. 1. Charge of the silica gel surface versus the pH of 1 M solutions of (*1*) $MgSO_4$, (*2*) $CaCl_2$, (*3*) Na_2SO_4, (*4*) LiBr, (*5*) water, and (*6*) $CuSO_4$.

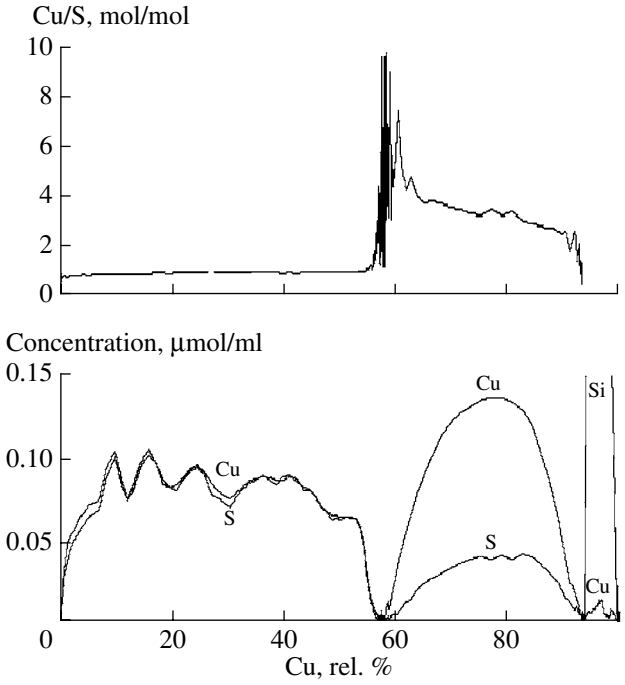

Fig. 2. Kinetics of Cu, S, and Si dissolution and the stoichiometry curve (Cu/S) of $CuSO_4$ (15.3 wt %)/SiO_2 in parametric form (relative to the degree of Cu dissolution).

etry in the temperature range 20–200°C at a vapor pressure of P_{H_2O} = 10–50 mbar on a Rigaki Thermoflex thermobalance. A weighed sample (15–20 mg) was placed in an isothermal air flow (100 cm^3/min) with a constant partial pressure of water vapor, and the equilibrium sorption of water vapor was detected from the weight change. Sorption was characterized by the number of moles of water sorbed by 1 mol of $CaCl_2$:

$$N(P_{H_2O}, T) = (m(P_{H_2O}, T)/\mu_{H_2O})/(m_s/\mu_s),$$

where $m(P_{H_2O}, T)$ is the equilibrium amount of water sorbed by the sample at the temperature T and the vapor pressure P_{H_2O}, m_s is the weight of the salt in the sample, and μ_{H_2O} and μ_s are the molar weights of water and salt.

RESULTS AND DISCUSSION

Adsorption of Metal Cations from a Solution on the Silica Gel Surface

The charge of the silica gel surface in salt solutions is a function of pH (Fig. 1). For pH > 6, the negative charge of the surface increases sharply due to the ionization of the silanol surface groups of the silica gel (reaction (I)). In salt solutions, the charge of the silica gel surface increases due to the formation of an electrical double layer and the adsorption of metal cations. The 3- to 10-fold increase in the surface charge in 1 M solutions of salts (Fig. 1) indicates that equilibria (II)–(IV) in solutions are shifted toward the formation of the surface complexes $\equiv Si–OM^{(n-1)+}$; that is, most of the negatively charged sites on the silica gel surface are compensated for by the metal cations adsorbed on the surface. Based on this assumption, we can estimate the amount of metal in the surface complexes $\equiv Si–OM^{(n-1)+}$. In neutral salt solutions (pH 5.5–6.5), the charge of the silica gel surface is 0.05–0.4 nm^{-2} (Fig. 1). The amount of metal adsorbed on the silica gel surface is estimated at 0.2–8 mg/g, depending on the salt. Metal cations have different adsorption capacities. As follows from our data (Fig. 1), cation adsorption on the silica gel surface increases in the order LiBr < Na_2SO_4 < $CaCl_2$ ≈ $MgSO_4$ < $CuSO_4$.

Chemical Composition

By way of example, we show the stoichiometry curve of the composite $CuSO_4$ (15.3 wt %)/SiO_2 (Fig. 2), which is typical of the sorbents examined. The metal cations in this composite exist in three different forms. One form is water-soluble, the second is soluble in hydrochloric acid, and the third can be dissolved only in hydrofluoric acid together with silica gel. These forms differ in terms of Cu/S molar ratio. In the water-soluble phase, the Cu/S ratio coincides with that in $CuSO_4$, being equal to 1. Evidently, this form represents metal incorporated into the stoichiometric $CuSO_4$ phase. Hereafter, this form will be called "free" for brevity.

The Cu/S ratio in the HCl-soluble phase changes during dissolution from 6–8 to 2. In our opinion, this phase represents surface complexes ("bound" cations) resulting from copper cation adsorption during the impregnation of the silica gel. The fact that Cu/S > 2 indicates that, along with $2(\equiv Si–OCu^+)SO_4^{2-}$ complexes, in which the copper cation is bonded to one silanol group, there are $2(\equiv Si–O^-)Cu^{2+}$ complexes, in

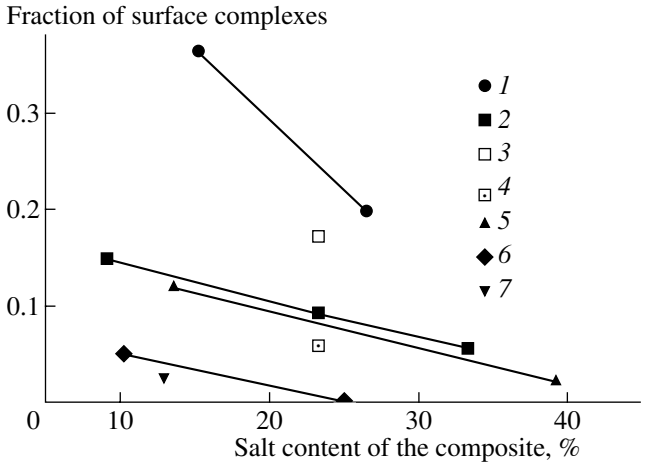

Fig. 3. Fraction of metal cations in the surface complexes versus the total salt content of the (*1*) $CuSO_4/SiO_2$, (*2–4*) $CaCl_2/SiO_2$, (*5*) $MgSO_4/SiO_2$, (*6*) Na_2SO_4/SiO_2, and (*7*) $LiBr/SiO_2$ composites synthesized from (*1*, *2*, *5–7*) neutral solutions and solutions with (*3*) pH 8 and (*4*) pH 1.

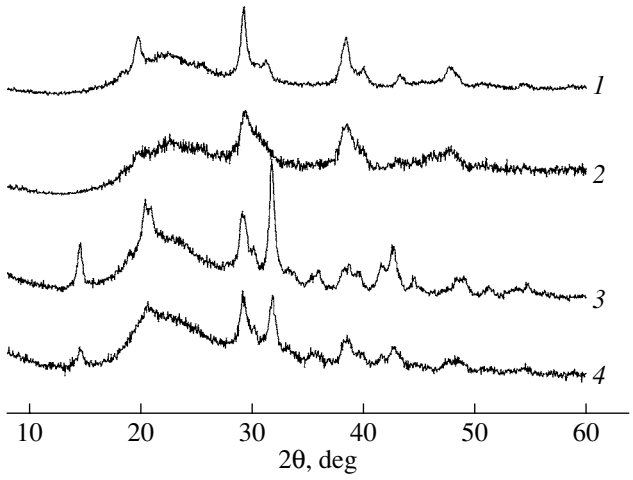

Fig. 4. X-ray diffraction patterns of $CaCl_2$ (23.3 wt %)/SiO_2 recorded at T = (*1*) 200 and (*2*) 370°C and (*3*, *4*, respectively) after cooling of these samples to T = 20°C.

which the copper cation is bonded to two silanol groups, or ≡Si–OCu^+OH^- complexes, which result from surface-induced hydrolysis.

Sulfur is absent from the phase that dissolves in hydrofluoric acid together with the silica gel. In our opinion, this form consists of the impurity metal present in the starting silica gel and, possibly, strongly bound surface complexes.

The results of the differentiating dissolution of the other samples are qualitatively similar. For instance, in all of the samples, the metal cations are in three different forms: a water-soluble salt phase, surface complexes soluble in HCl, and impurities in silica gel.

The fractions of bound and free cations differ for composites based on different salts (Fig. 3). The fraction of bound cations increases in the order LiBr < Na_2SO_4 < $CaCl_2$ ≈ $MgSO_4$ < $CuSO_4$. This order coincides with the order derived from potentiometric data. Note that the metal concentration in the surface complexes is 0.3–10 mg/g for different composites, which is close to the amount of adsorbed metal estimated from potentiometric titration data (0.2–8 mg/g).

To ascertain that the formation of bound metal in the composites is related to the adsorption of metal cations on the silica gel surface at the impregnation stage, we synthesized $CaCl_2$ (23.3 wt %)/SiO_2 sorbents, shifting the ion-exchange equilibrium (reactions (II)–(IV)) to the right or left by varying the pH of the impregnating solution. The results of the differentiating dissolution of these composites (Fig. 3) show that the fraction of calcium in the surface complexes increases from 0.09 to 0.16 with an increase in the pH of the solution from 5.5 to 8. On the contrary, reducing the pH to 2 decreases the metal fraction in the complexes to 0.04.

Thus, metal cation adsorption from salt solutions on the silica gel surface at the impregnation stage produces two different forms of the metal in the composite sorbents: part of the metal appears in the stoichiometric salt phase in silica gel pores, and part appears in complexes on the silica gel surface. The shift of the ion-exchange equilibrium (reactions (II)–(IV)) at the impregnation stage toward cation adsorption as a result of the increase in pH causes an increase in the proportion of bound metal cations.

Phase Composition

The SSGP composites contain two salt phases in their pores: part of the salt forms a surface amorphous phase, and part forms a bulk crystalline phase [11, 12]. The surface amorphous salt results from the interaction between the salt and silica gel surface. However, the mechanism of this interaction was unknown. To study the influence of the two possible mechanisms of interaction (cation adsorption and solid-phase spreading) on the phase composition of the composites, the parameters affecting these processes (the pH of the impregnating solution and drying temperature) were varied during the synthesis of the $CaCl_2/SiO_2$ composites.

Figure 4 illustrates the influence of drying temperature on the phase composition of $CaCl_2/SiO_2$. The X-ray diffraction patterns from this composite recorded at 200 and 370°C contain peaks corresponding to the anhydrous salt $CaCl_2$. However, the peak widths and intensities in these patterns differ. As the temperature is raised, the reflections broaden and their intensity decreases. This suggests that the coherently scattering region diminishes or the salt phase undergoes disordering and grows finer. Perhaps, part of the salt is converted into an X-ray amorphous state. It is most likely that the Coulomb interaction between salt ions and the silica gel surface induces the disordering of the crystal structure of the salt particles and the formation of a disordered or

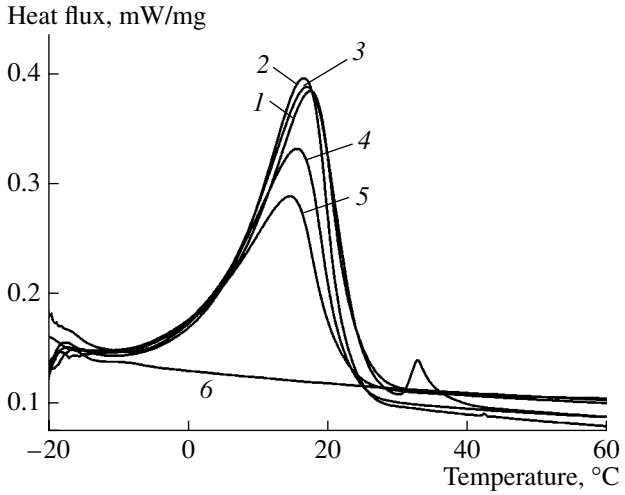

Fig. 5. Thermoanalytical curves for $CaCl_2$ (23.3 wt %)/SiO_2 calcined at T = (*1*) 170, (*2*) 220, (*3*) 270, (*4*) 320, (*5*) 370, and (*6*) 470°C.

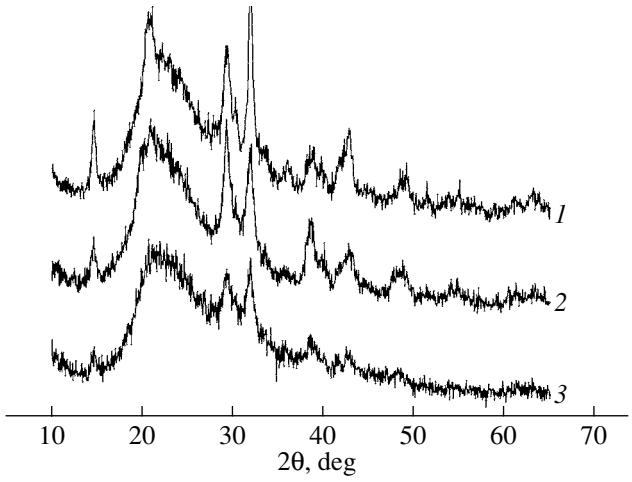

Fig. 6. Thermoanalytical curves for $CaCl_2$ (23.3 wt %)/SiO_2 synthesized using impregnating solutions with (*1*) pH 1, (*2*) pH 5.5, and (*3*) pH 8.

amorphous salt phase on the silica gel surface through solid-phase salt spreading [16, 17], thus compensating for the excess surface energy of the salt nanoparticles. Raising the drying temperature increases the mobility of the salt ions and favors the solid-phase salt spreading over the silica gel surface.

Upon the cooling of the composites to room temperature, $CaCl_2$ is transformed into the hydrate $CaCl_2 \cdot 2H_2O$ through water vapor adsorption. The intensities of reflections from $CaCl_2 \cdot 2H_2O$ depend on the sample pretreatment temperature. For the sample calcined at 370°C, in which the degree of crystallinity of the salt is lower, the reflections from $CaCl_2 \cdot 2H_2O$ are weaker. This is due to the fact that the sorption of water vapor by the crystalline salt yields crystalline hydrates, while the sorption of vapor by the disordered or X-ray amorphous salt phase results in an X-ray amorphous hydrate.

Differential scanning calorimetry data for composites calcined at different temperatures are presented in Fig. 5 as melting curves of $CaCl_2 \cdot 6H_2O$. For drying temperatures below 270°C, the melting peak of $CaCl_2 \cdot 6H_2O$ in the composite is invariable. As the drying temperature is further raised, the melting peak decreases. This is caused by the amorphization of part of the salt. No melting peak is observed for the composite calcined at T = 470°C, indicating that the salt in this composite is entirely amorphous. Thus, for drying temperatures above 270°C, the solid-phase spreading of calcium chloride over the silica gel surface is significant and produces a disordered or amorphous surface phase.

The effect of the pH of the impregnating solution on the phase composition of the composite is demonstrated in Fig. 6. The X-ray diffraction patterns from the composites $CaCl_2$ (23.2 wt %)/SiO_2 synthesized at different pH contain reflections from the crystalline phase $CaCl_2 \cdot 2H_2O$ (the analysis was carried out at room temperature, at which anhydrous $CaCl_2$ is converted into $CaCl_2 \cdot 2H_2O$). The integrated intensity of the peaks differs substantially from sample to sample. An increase in the pH of the impregnating solution, shifting equilibria (II)–(IV) toward cation adsorption, induces a decrease in the peak intensity. This indicates that part of the salt is converted into an X-ray amorphous phase. Using a mechanical mixture of calcium chloride and silica gel as the reference sample, we estimated the amount of the crystalline salt in the samples. In the $CaCl_2$ (23.3 wt %)/SiO_2 composites synthesized at pH 1, 5.5, and 8, the amount of this phase is 21, 13, and 7 wt %, respectively. Thus, in the specimens synthesized at pH 5.5 and 8, the amount of crystalline $CaCl_2$ is much lower than the total salt content of the composite.

The differential scanning calorimetry data for $CaCl_2/SiO_2$ composites synthesized at different pH values are confirmed by X-ray diffraction data (Fig. 7). The strength of the $CaCl_2 \cdot 6H_2O$ melting peak depends on the pH of the solution at the impregnation stage. An increase in the pH of the salt solution from 1 to 5.5 reduces the melting peak. No $CaCl_2 \cdot 6H_2O$ melting peak is observed for the specimen synthesized at pH 9. This indicates that all of the salt in this specimen is in the amorphous state.

Thus, the phase composition of the composite depends on the adsorption of calcium cations on the silica gel surface at the impregnation stage and on the composite drying temperature. Shifting the ion-exchange equilibrium toward cation adsorption favors the formation of the amorphous salt in silica gel pores. It is most likely that the surface complexes resulting from cation adsorption at the impregnation stage serve as nucleation centers for salt crystals at the drying stage. Raising the pH increases the amount of surface complexes, favoring the formation of the salt as clusters of atomic sizes or as an amorphous film on the silica gel surface.

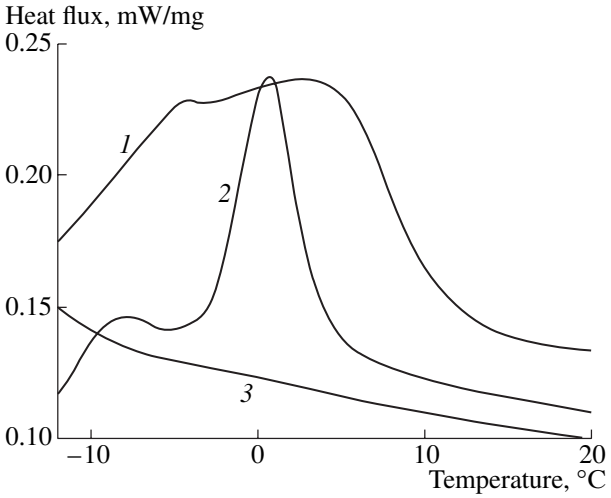

Fig. 7. Thermoanalytical curves for $CaCl_2$ (23.3 wt %)/SiO_2 synthesized using impregnating solutions with (*1*) pH 1, (*2*) pH 5.5, and (*3*) pH 9.

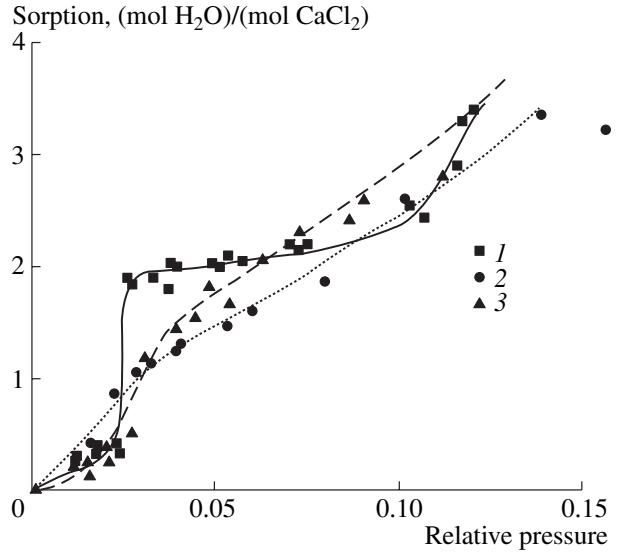

Fig. 8. Temperature invariant curves for water vapor sorption by $CaCl_2$ (33.4 wt %)/SiO_2 synthesized using impregnating solutions with (*1*) pH 5.5, (*2*) pH 8, and (*3*) pH 5.5 at T = (*1*, *2*) 200 and (*3*) 370°C.

Sorption Properties of the Composite Sorbents

Modifying synthesis conditions not only alters the chemical and phase compositions of the composites but also results in qualitative changes in the sorption equilibrium between the composites and water vapor. Figure 8 demonstrates the influence of the pH of the impregnating solution and of the drying temperature on the sorption equilibrium between $CaCl_2$ (33.4 wt %)/SiO_2 and water vapor.

A characteristic feature of the vapor sorption isotherm for $CaCl_2$ (33.4 wt %)/SiO_2 synthesized at pH 5.5 and dried at 200°C is a plateau at a sorption value of $N = 2$. The value of N remains unchanged at relative vapor pressures of $\eta = 0.03$–0.09, indicating the formation of the stable crystalline hydrate $CaCl_2 \cdot 2H_2O$, which is also typical of the bulk $CaCl_2 \cdot H_2O$ system [5, 20]. At $\eta < 0.03$, the crystalline hydrate decomposes in steps to anhydrous calcium chloride. At $\eta > 0.09$, the sorption curve ascends monotonically with increasing humidity, indicating the formation of an aqueous solution of $CaCl_2$ in the pores [5, 20].

The plateau is absent from the vapor sorption curve for $CaCl_2/SiO_2$ synthesized at pH 8 and 200°C. The composition of this system changes monotonically throughout the sorption range (N = 0–6). In other words, no stable crystalline hydrate forms in this composite. This type of sorption equilibrium is characteristic of solutions of salts [9, 20] or hydrates with a "vacancy" structure [10].

Similar changes in the vapor sorption equilibrium are induced by an increase in the composite drying temperature. For instance, the isotherm of the specimen dried at $T = 370$°C has no plateau corresponding to the formation of $CaCl_2 \cdot 2H_2O$ in the pores. The sorption curve of this specimen ascends monotonically with increasing humidity.

Thus, for the composite $CaCl_2/SiO_2$, raising the pH of the impregnating solution and the drying temperature, which favors the formation of an amorphous salt in the pores of KSK silica gel, changes the type of composite–water vapor sorption equilibrium as well.

CONCLUSION

The ion-exchange interaction between a salt solution and the silica gel surface at the synthesis stage produces $\equiv Si–OM^{(n-1)+}$ surface complexes, which are likely to serve as nucleation centers for salt crystals at the composite drying stage. As a consequence, they affect the formation of salt phases in the silica gel pores. As a result, the crystalline and X-ray amorphous phases of the salt are formed. Shifting the ion-exchange equilibrium toward cation adsorption decreases the amount of the crystalline phase and increases the proportion of amorphous salt in the $CaCl_2/SiO_2$ composite. An increase in the composite drying temperature above 270°C also favors the formation of the amorphous phase through the solid-phase spreading of the salt over the silica gel surface. The character of the sorption equilibrium between the composite sorbents and water vapor depends on the phase composition of the composite. In the sorbents dominated by the crystalline salt, the crystalline hydrate $CaCl_2 \cdot 2H_2O$, with a fixed composition, forms during vapor sorption. The composition of the sorbents dominated by the X-ray amorphous salt changes continuously during vapor sorption. This behavior is typical of solutions and crystalline hydrates of the vacancy type. No stable crystalline hydrates form in these sorbents. Varying the composite synthesis con-

ditions allows the composite–water vapor sorption equilibrium to be controlled.

ACKNOWLEDGMENTS

The authors thank T.A. Kriger for the X-ray diffraction examination of the composites.

This work was supported in part by the INTAS (grant no. 2003-51-6260), the Russian Foundation for Basic Research (project nos. 03-02-39017, 04-02-81028, and 05-02-16953), and the Integration Project of the Siberian Division of the Russian Academy of Sciences (grant no. 133).

REFERENCES

1. Nedeljkovic, J.M., *Mater. Sci. Forum*, 2000, vol. 352, p. 79.
2. Kryszewski, M., *Synth. Met.*, 2000, vol. 109, nos. 1–3, p. 47.
3. Aristov, Yu.I., Tokarev, M.M., Di Marko, G, Kachchiola, G., Restuchcha, D., and Parmon, V.N., *Zh. Fiz. Khim.*, 1997, vol. 71, no. 2, p. 253.
4. Tokarev, M.M., Kozlova, S.G., Gabuda, S.P., and Aristov, Yu.I., *Zh. Strukt. Khim.*, 1998, vol. 39, no. 2, p. 259.
5. Aristov, Yu.I., Tokarev, M.M., Cacciola, G., and Restuccia, G., *React. Kinet. Catal. Lett.*, 1996, vol. 59, no. 2, p. 325.
6. Gordeeva, L.G., Restuchcha, D., Kachchiola, G., and Aristov, Yu.I., *Zh. Fiz. Khim.*, 1998, vol. 72, no. 7, p. 1236.
7. Gordeeva, L.G., Restuchcha, D., Tokarev, M.M., Kachchiola, G., and Aristov, Yu.I., *Zh. Fiz. Khim.*, 2000, vol. 74, no. 12, p. 2211.
8. Gordeeva, L.G., Resstuccia, G., Freni, A., and Aristov, Yu.I., *Fuel Process. Technol.*, 2002, vol. 79, no. 3, p. 225.
9. Aristov, Yu.I., Tokarev, M.M., Cacciola, G., and Resstuccia, G., *React. Kinet. Cat. Lett.*, 1996, vol. 59, no. 2, p. 325.
10. Mutin, J.C., Watelle, G., and Dusausoy, Y., *J. Solid State Chem.*, 1979, vol. 27, no. 3, p. 407.
11. Gordeeva, L.G., Glaznev, I.S., and Aristov, Yu.I., *Zh. Fiz. Khim.*, 2003, vol. 77, no. 10, p. 1906.
12. Gordeeva, L.G., Glaznev, I.S., Malakhov, V.V., and Aristov, Yu.I., *Zh. Fiz. Khim.*, 2003, vol. 77, no. 11, p. 2048.
13. Iler, R.K., *The Chemistry of Silica*, New York: Wiley, 1979.
14. Jang, H.M. and Fuerstenau, D.W., *Colloids Surf.,* 1986, vol. 21, p. 235.
15. Greenberg, S.A., *J. Phys. Chem.*, 1956, vol. 60, no. 3, p. 325.
16. Maier, J., *J. Phys. Chem. Solids*, 1985, vol. 46, no. 3, p. 309.
17. Uvarov, N.F., *Zh. Prikl. Khim.*, 2000, vol. 73, no. 6, p. 970.
18. Malakhov, V.V., *J. Mol. Catal. A*, 2000, vol. 158, no. 1, p. 143.
19. Vasilyeva, I.G., Malakhov, V.V., Dovlitova, L.S., and Bach, H., *Mater. Res. Bull*, 1999, vol. 34, no. 1, p. 81.
20. *Gmelins Handbuch der anorganischen Chemie: Calcium*, Weinheim: Chemie, 1957.